Evidence for pressure-induced node-pair annihilation in Cd₃As₂

Cheng Zhang,[1,2] Jianping Sun,[3] Fengliang Liu,[1,2,4] Awadhesh Narayan,[5,6] Nana Li,[4] Xiang Yuan,[1,2] Yanwen Liu,[1,2]
Jianhong Dai,[3] Youwen Long,[3,7] Yoshiya Uwatoko,[8] Jian Shen,[1,2,9] Stefano Sanvito,[6] Wenge Yang,[4,10,*]
Jinguang Cheng,[3,†] and Faxian Xiu[1,2,9,‡]

[1]*State Key Laboratory of Surface Physics and Department of Physics, Fudan University, Shanghai 200433, China*
[2]*Institute for Nanoelectronic Devices and Quantum Computing, Fudan University, Shanghai 200433, China*
[3]*Beijing National Laboratory for Condensed Matter Physics and Institute of Physics, Chinese Academy of Sciences, Beijing 100190, China*
[4]*Center for High Pressure Science and Technology Advanced Research (HPSTAR), Shanghai 201203, China*
[5]*Department of Physics, University of Illinois at Urbana-Champaign, Urbana, Illinois 61801, USA*
[6]*School of Physics and CRANN and AMBER, Trinity College, Dublin 2, Ireland*
[7]*Collaborative Innovation Center of Quantum Matter, Beijing 100190, China*
[8]*Institute for Solid State Physics, University of Tokyo, Kashiwa, Chiba 277-8581, Japan*
[9]*Collaborative Innovation Center of Advanced Microstructures, Nanjing, 210093, China*
[10]*High Pressure Synergetic Consortium (HPSynC), Geophysical Laboratory, Carnegie Institution of Washington,
Argonne, Illinois 60439, USA*

We report a magnetotransport study of Dirac semimetal Cd₃As₂ under high pressure. The Shubnikov–de Haas oscillations are measured at different pressures to reveal the evolution of the Fermi surface. A sudden change in the phase factor of the oscillations occurs at 1.3 GPa along with the unanticipated shrinkage of the Fermi surface, which is well below the structure transition point from the tetragonal to the monoclinic structure (∼2.5 GPa). High-pressure x-ray diffraction also reveals an anisotropic compression of the Cd₃As₂ lattice around a similar pressure. Through the first-principles calculations, we find that such axial compression along the c direction will shift the Dirac nodes towards the Brillouin zone center and will eventually introduce a finite energy gap. Our result unveils a possible topological phase transition in pressurized Cd₃As₂ without structure transition.

I. INTRODUCTION

Playing an important role in the topological phase diagram, Dirac semimetals can serve as a parent phase and be driven into many other exotic states, like Weyl semimetals or topological insulators, by explicitly breaking certain symmetries [1–3]. Recently, there has been a surge of interest in the phase transition of topological semimetals, as studied theoretically [1,4–10]. Many exotic physical phenomena, such as quantum criticality [4,8], metal-insulator transitions [7], and evolution of Fermi arc states [9], have been predicted to emerge at the critical transition points of topological semimetals. Despite the theoretical progress, these topological phase transitions remain largely unexplored through experimental study. The difficulty lies in finding a way to effectively tune the electronic states across the topological phase transition. Evidence of a phase transition from a Dirac semimetal to a gapped phase has only been found in the Dirac semimetal Cd₃As₂ under high magnetic field [3,11]. However, a complex interplay between different kinds of symmetry breaking will emerge under such a circumstance since the magnetic field deviating from the crystal rotational axis breaks both the C_4 and the time-reversal symmetry. Furthermore, the large g factor in Cd₃As₂ also contributes to a strong spin-orbit coupling with magnetic field [12]. Hence, a neat and more straightforward

method of inducing topological phase transition in experiments remains to be discovered.

As widely used in condensed matter physics and geoscience, the application of high pressure provides a clean and effective means to modulate the physical and chemical properties of materials [13]. By directly tuning the lattice constant, high pressure can drastically impact the electronic structure even for strongly correlated materials with high carrier density, which is hard to achieve through other methods, for instance, electrostatic gating. Many interesting physical phenomena, such as quantum criticality and unconventional superconductivity, have been intensively studied under pressure [14,15]. Unfortunately, several topological semimetals, including NbAs [16,17], TaAs [18], and NbP [19], were reported to behave as a strong crystalline lattice, where the external pressure over a moderate range cannot easily tune the Fermi surface (FS) and the band structure. Meanwhile, their complicated band structures make the detailed analysis of FS through the Shubnikov–de Haas (SdH) oscillations rather difficult. In contrast, Cd₃As₂ has been shown to exhibit remarkable changes in transport properties by applying pressure or stress [20–23]. A structural phase transition from a metallic tetragonal phase to a semiconducting monoclinic one at around 2.57 GPa has been reported in Cd₃As₂ [20]. With the pressure further increased to 8.5 GPa, a superconducting transition emerges with T_c around 2 K [23]. Similarly, the signature of unconventional superconductivity has also been reported by point-contact-induced local stress [21,22]. These studies prove the validity of using pressure as a tuning tool of the band structure in Cd₃As₂. Nevertheless, it is still unclear how the FS evolves under external pressure, a

*yangwg@hpstar.ac.cn
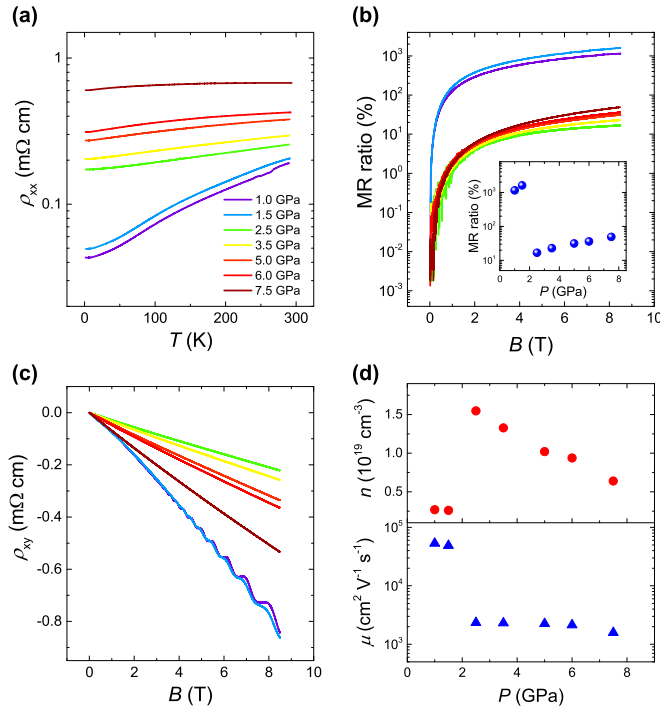†jgcheng@iphy.ac.cn
‡faxian@fudan.edu.cn

FIG. 1. High-pressure transport measurements across the structure transition in sample T1. (a) The temperature dependence of resistivity (R-T) curve under different pressures. (b,c) The magnetic field dependence of MR ratio (b) and Hall resistivity (c) under different pressures at 2 K. The inset of (b) is the MR ratio at 8.5 T. (d) The carrier density n and mobility μ at 2 K under different pressures.

crucial aspect for a better understanding of these intriguing phenomena.

II. RESULTS AND DISCUSSION

Here, we report a systematic magnetotransport and x-ray diffraction (XRD) study of Cd_3As_2 under hydrostatic pressures to reveal the evolution of electronic structure. Figure 1(a) shows the temperature-dependent resistivity (R-T) curves of sample T1 under different pressures P. The resistivity of Cd_3As_2 increases with pressure in the 1.0–7.5 GPa range. A clear transition in the slope of the R-T curve takes place at 2.5 GPa, corresponding to the structural transition from a tetragonal phase to a monoclinic one [20]. Such a clear difference can also be found in the magnetoresistivity (MR) ratio as shown in Fig. 1(b). The MR ratio at 8.5 T decreases by nearly two orders of magnitude after the transition [Fig. 1(b), inset]. The Hall resistivity ρ_{xy} at 2 K [Fig. 1(c)] exhibits a linear dependence on the magnetic field **B** both before and after the structural transition. By analyzing the Hall effect, we can determine the pressure dependence of the carrier density and the mobility [Fig. 1(d)]. The carrier density abruptly increases from 2.5×10^{18} to 1.5×10^{19} cm^{-3} at 2.5 GPa, followed by a continuous decrease at higher pressure. The high carrier density explains the metalliclike R-T curves in the high-pressure monoclinic phase [20]. The mobility in sample T1 is around 53000 cm^2/V s at low temperature in the tetragonal phase, similar to other transport experiments

on Cd_3As_2 [3,24–28]. The mobility decreases by over 20 times after the structure transition. This strong decreasing trend of mobility is consistent with the previous report [20]. Accordingly, the SdH oscillations disappear immediately after the transition.

In order to elucidate how the band structure evolves within the tetragonal phase, we systematically measured the magnetotransport of sample T2 (0–2.17 GPa). The pure oscillations have been analyzed by subtracting a polynomial background from the MR. The extracted SdH oscillations are plotted as a function of $1/B$ and P in Fig. 2(a). The peaks and valleys of the oscillations are periodic in $1/B$ and can be clearly tracked at different pressures. By employing fast Fourier transform (FFT) analysis, we can determine the oscillation frequency F. The frequency of SdH oscillations corresponds to a closed cyclotron orbit in k space, described by $F = (\phi_0/2\pi^2)S_F$ with $\varphi_0 = h/2e$. Here S_F is the extremal cross-section area of the FS. Figure 2(b) summarizes the FFT spectra of the SdH oscillations at different P. The persistent single peak feature at different pressures indicates that only one cyclotron orbit (or several degenerate ones) contributes to the oscillations, similarly to the previous reports [3,26]. A distinct behavior is that the oscillation frequency becomes smaller towards higher pressure. Conventionally, the FS tends to increase upon compression due to the decrease of the gap size or the overlapping of the bands [29–32]. However, the anomalous decrease of FS with pressure suggests that the band structure experiences unexpected changes other than the pure lattice shrinkage effect. By assuming an isotropic three-dimensional FS (which is indeed the case for Cd_3As_2 at ambient pressure), we can calculate the Fermi wave vector at different pressures as shown in Fig. 2(c). Here the carrier density given by the SdH oscillations is $n = \frac{k_F^3}{3\pi^2} \approx 1.9 \times 10^{18}$ cm^{-3} with the spin degeneracy of 2 taken into consideration. This value is close to the Hall carrier density of 2.6×10^{18} cm^{-3}. The Fermi energy is also estimated based on the dispersion relationship determined in other studies [12,33,34]. A Lifshitz transition takes place at around $E_{Lif} \approx 20$ meV above the Dirac points (corresponding to $k_{Lif} \approx 0.003$ Å^{-1}) [35]. This clearly shows that the Fermi level is still well above the Lifshitz transition up to 2.17 GPa.

The Berry phase is a phase difference acquired over a closed path in the parameter space during a cyclic adiabatic process [36]. Cyclotron orbits that enclose a Dirac point have been found to result in a nontrivial π Berry phase [36,37]. This semiclassical Berry phase can be detected by the phase factor of quantum oscillations through the relation $\gamma = 1/2 - \phi_B/2\pi$. The π Berry phase in the quantum oscillation is in fact a direct consequence of the Dirac-type Landau level spectrum [38–40]. Among different studies, the quantum oscillation data in Cd_3As_2 consistently point to a nearly nontrivial phase factor γ ($\gamma = 0$ when resistance peaks are assigned integer Landau levels as, or $\gamma = 0.5$ when, valleys are integer) [3,24,25,41]. However, in Cd_3As_2, the Fermi level is usually located well above the Lifshitz energy where the FS encloses two Dirac points [12,26,33]. Thus theoretically it should exhibit an overall phase of 0.

Now let us revisit the band structure of Cd_3As_2. In Cd_3As_2, despite the high doping level, the dispersion near the Fermi
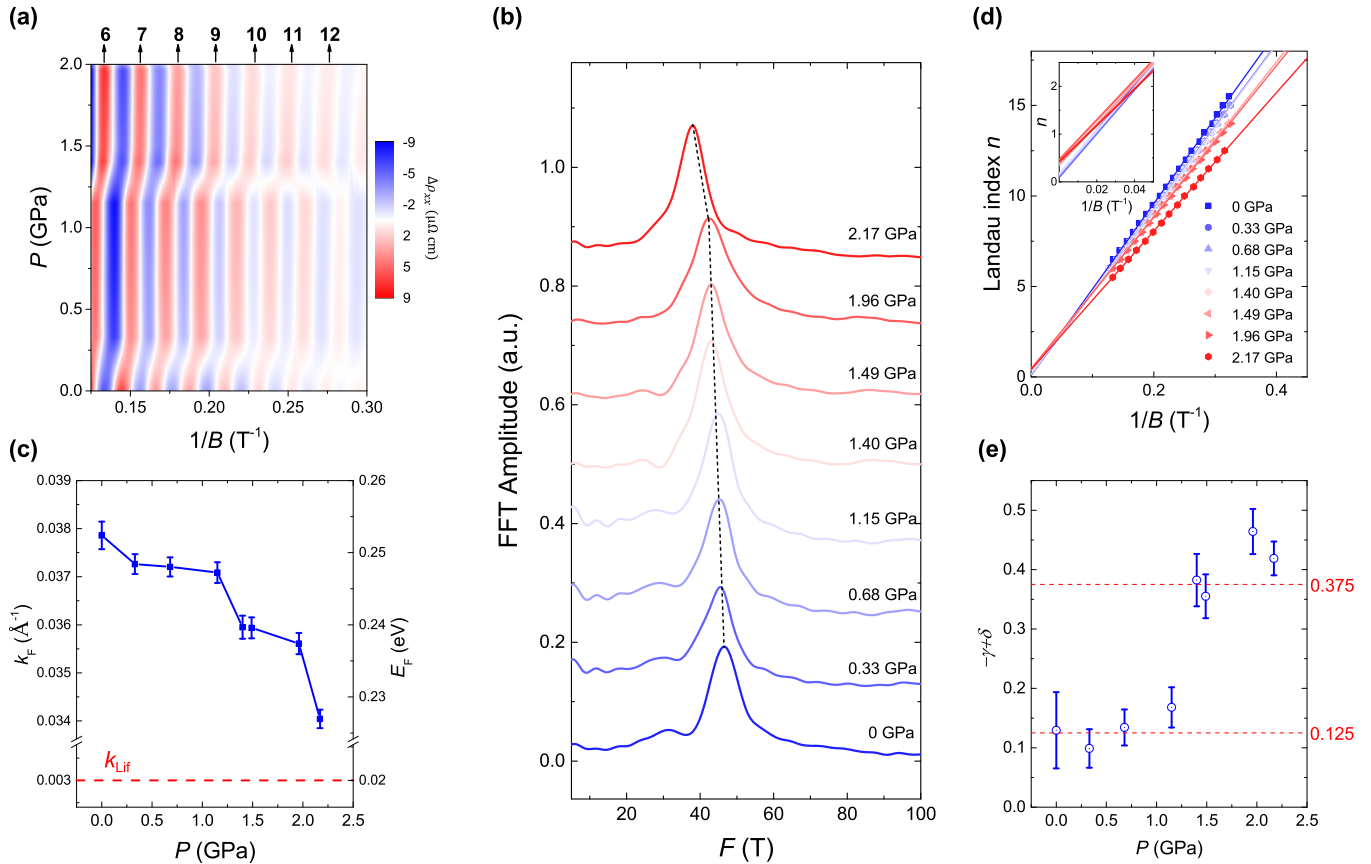
FIG. 2. The pressure dependence of SdH oscillations in sample T2. (a) The extracted SdH oscillations as a function of $1/\boldsymbol{B}$ and pressure at 2 K. The peaks are marked as a series of the Landau level index. (b) A stack view of the FFT spectrum of SdH oscillations at different pressures. (c) The pressure dependence of Fermi wave vector k_F. The corresponding Fermi wave vector k_{Lif} and Fermi level E_F for Lifshitz transition is based on calculations at ambient pressure. (d) The Landau fan diagram of sample T2 under different pressures. The inset of (d) is a close look at the y-axis intercept. (e) The extracted phase factor $-\gamma + \delta$ under different pressures.

energy remains to be linear as demonstrated in the previous experiments [12,33,34]. It means that the overall band structure of Cd_3As_2 cannot be simply modeled by the crossing of quadratic bands. The origin of the linear dispersion at large energy scale was later interpreted as the coexistence of massless Kane and Dirac fermions as described by the Bodnar model [42]. Band structure at large energy mainly follows a Kane mode (also with linear dispersion) and the Dirac physics is hidden in a very low energy scale below the Lifshitz energy. Near the band edge, the dispersion evolves from linear to quadratic behavior. Such quadratic component at low energies is deformed from the flat band in a standard Kane model when introducing the crystal field splitting term [42]. Therefore, the observed Berry phase is actually contributed by the Kane fermion. The Landau level energy of the Kane fermion takes a similar form of field dependence but differs in the zeroth Landau level and spin splitting [43]. As a result of its unique Landau level spectrum, the Berry phase of the Kane model is non-π-quantized unlike massless Dirac systems and varies with model parameters, gap size, and spin-orbit coupling [44]. It also differs from the conventional systems with a quadratic band in which the Berry phase is always trivial. In Fig. 2(d), we have performed a linear fit to the peak and valley positions as a function of $1/\boldsymbol{B}$ as integer and half integer, respectively. There is a clear trend of the y-axis offset with pressure in

the Landau fan diagram [Fig. 2(d), inset, and Fig. 2(e)]. The intercept $-\gamma + \delta$ experiences a sudden jump around 1.3 GPa from ~ 0.13 at lower pressure to ~ 0.42 at higher pressure up to 2.17 GPa. Here δ is an additional phase shift from the FS curvature, which only changes with the shape of FS [45]. Thus the shift of the phase factor comes from the Berry phase. In our case, the pressure regime should not have a significant impact on the spin-orbit coupling, which remains largely determined by the material itself. Therefore, the most likely case is that the energy gap of the Kane fermion is tuned by the pressure. It modifies the band dispersion near the Fermi surface therefore leads to the shift of phase offset in quantum oscillation. The band structure calculated with the Bodnar model in the previous study [42] also indicates that the band dispersion can be largely modified by the standard Kane parameters like band gap, which could be effectively tuned through pressure. A similar case also happens in massive Dirac systems where the Berry phase changes continuously from π to 0, depending on the gap size and the Fermi energy [39,40]. Such a finite gap effect should be further enhanced in strongly particle-hole asymmetric systems, like Cd_3As_2. Currently it is difficult to perform a quantitative analysis of the evolution of the Bodnar model through the transport data. Further investigation could be made through optical methods combined with high pressure.
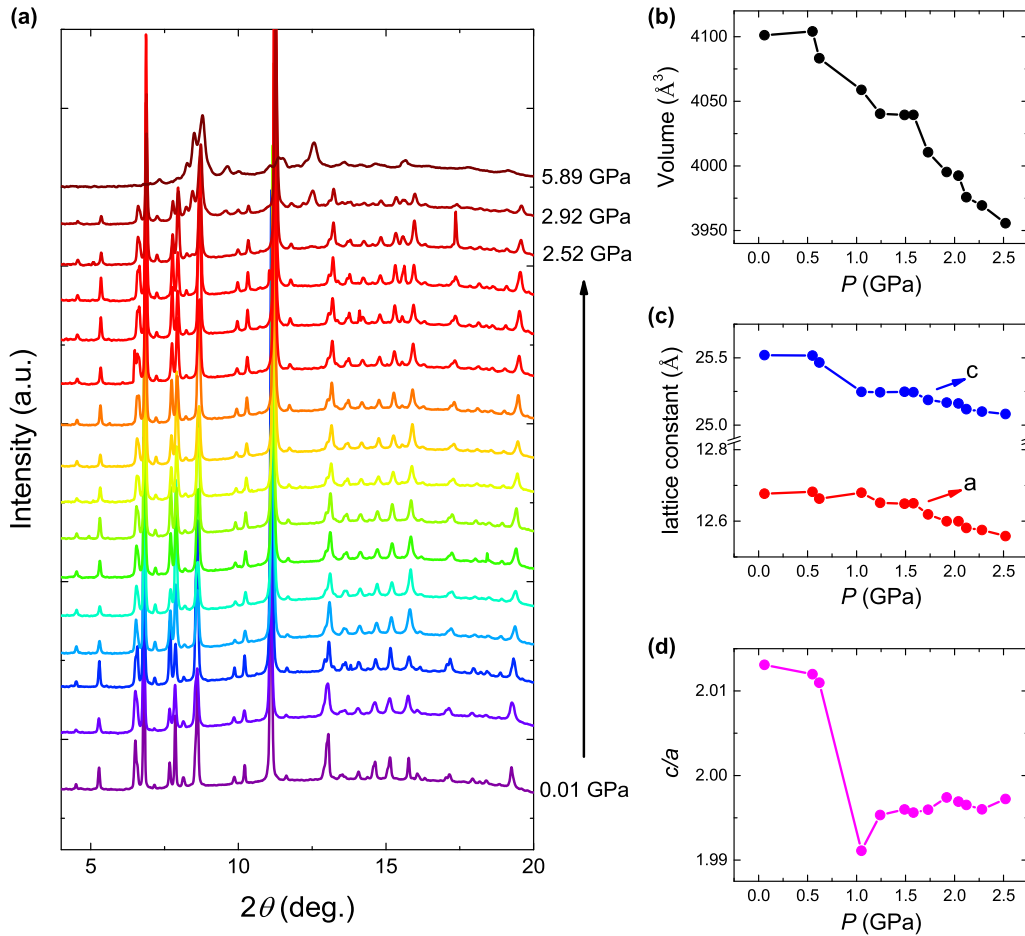
FIG. 3. The high-pressure XRD study of Cd_3As_2. (a) A stack view of the XRD spectrum under different pressures. (b) The pressure dependence of unit cell volume, (c) the lattice constants a and c, and (d) the lattice constant ratio c/a extracted within the tetragonal phase. Here the error bars of the lattice constant given by the XRD fitting software are below 0.01 Å, almost negligible. By carefully checking the fitted parameters, the fluctuation of the lattice constant value is found to be below 0.04 Å, five times smaller than the sudden jump of c ($\sim$0.23 Å) at 1 GPa. The critical pressure of XRD and transport is slightly different possibly due to the different temperatures at which the pressures were calibrated (room temperature for XRD and below 10 K for transport).

In order to figure out how pressure may affect the band structure, we carried out high-pressure synchrotron XRD experiments with a symmetric diamond anvil cell. We note that owing to the experimental limitation, the XRD experiments were performed at room temperature, different from that of quantum oscillation measurements at 2 K. Figure 3(a) presents the angle-dispersive XRD patterns of Cd_3As_2 under different pressures. Similar to previous reports [20], the XRD spectrum experiences a significant change at 2.92 GPa, corresponding to the tetragonal to monoclinic structure transition. In the pressure range of 0.01–0.92 GPa, the XRD patterns show no significant changes with peaks systematically moving towards the higher angles. We performed Rietveld refinement to unveil the evolution of the tetragonal lattice structure in Cd_3As_2 under pressure. The obtained lattice parameters as a function of pressure are plotted in Figs. 3(b)–3(d). Both the unit-cell volume [Fig. 3(b)] and the lattice constants [Fig. 3(c)] decrease with increasing pressure. However, at around 1 GPa, the lattice constant c experiences an abrupt contraction, which is absent in the volume and the lattice constant a. Considering the fact that the XRD results can be still well fitted by

the tetragonal structure, the transition here should be an isostructural transition rather than a strong transformation between different point groups. Thus the C_4 symmetry is still preserved. The c/a ratio shown in Fig. 3(d) further reveals this anomalous transition. The ratio remains nearly unchanged in the regimes of 0.01–0.62 GPa and 1.24–2.52 GPa, but presents a steplike feature at around 1 GPa. The Cd_3As_2 crystal exhibits different changes along the $a(b)$ direction and the c direction, suggesting an anisotropic-compression behavior. We note that the data fluctuation between fitted lattice constant values is below 0.04 Å, which does not affect the overall trend of lattice constants vs pressure nor the large step observed here.

To study the influence of the anisotropic compression on the band structure, we carried out first-principles calculations within density functional theory using the Vienna *Ab-Initio* Simulation Package (VASP) [46]. The Perdew-Burke-Ernzerhof form of the exchange-correlation functional was used [47]. A plane-wave cutoff of 300 eV was employed and the Brillouin zone was sampled using a $4 \times 4 \times 2$ k-point grid. Spin-orbit coupling was included in all calculations. Experimentally obtained lattice parameters were used. We
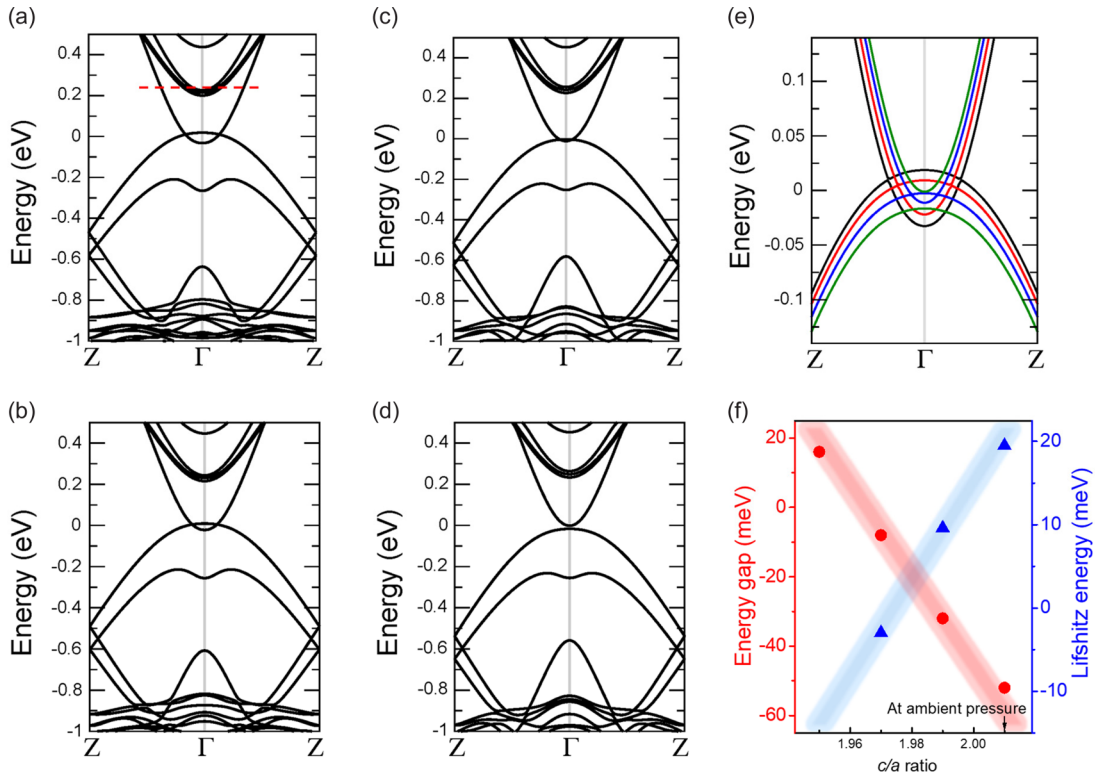
FIG. 4. First-principles band structure for Cd_3As_2 at different c/a ratios. (a–d) The calculated band structure with the c/a ratio being 2.01 (a), 1.99 (b), 1.97 (c), and 1.95 (d), respectively. The red dashed line in (a) corresponds to the position of the Fermi level at ambient pressure. (e) Zoom around the Dirac points comparing the band structures at the different c/a ratios. Black, red, blue, and green curves correspond to (a–d), respectively. (f) The evolution of the energy gap at Γ point and Lifshitz energy with decreasing c/a ratio. The negative value of the energy gap corresponds to an inverted band. Note that the Lifshitz transition is absent when a positive energy gap is generated.

considered several values of the c/a ratio, starting from $c/a = 2.01$, which is the ambient pressure value, going down to $c/a = 1.95$. The band structures for the different cases are shown in Figs. 4(a)–4(d). As expected, for $c/a = 2.01$, there is a Dirac crossing along the Γ-Z direction, which closely matches previous reports [48]. With decreasing c/a we notice that the Dirac nodes shift closer to the Brillouin zone center, becoming nearly overlapping for $c/a = 1.97$. On further lowering c/a to 1.95, the time-reversed Dirac partners annihilate and a band gap around 20 meV opens up [Fig. 4(e)]. Figure 4(f) summarized the trend of the energy gap and Lifshitz energy from the calculated band structure when decreasing c/a ratio. A systematic transition from an inverted band to a normal one will take place as c/a decreases. In order to further support the evolution of the band structure, a low-energy model with anisotropic compression has been provided in the Supplemental Material [49] by introducing a mass term m_0 into the effective Hamiltonian. As m_0 subsequently changes sign, a band gap is created. The effect of anisotropic compression is precisely that of reducing the mass inversion strength and can be mimicked by tuning the parameter m_0 in the low-energy model. Remarkably, this is similar to the effect of alloying Cd_3As_2 with a lighter element, which also causes such a motion and annihilation of Dirac points [50]. Despite the slight difference of the critical c/a value given by theory and experiments, we found that their overall decreasing trend of energy gap when reducing c/a is quite similar. Moreover, the anomalous shrinkage of the FS

[Figs. 2(b) and 2(c)] observed in experiments also supports the calculated band structure. Moreover, it is consistent with the observed increase of resistance with pressure within the tetragonal structure as reported previously [20]. Note that here we only focus on the effect of the c/a ratio on the band structure since it takes place at a pressure similar to that where the Berry phase in the transport suddenly changes. For comparison, another set of calculations by assuming isotropic compression was also performed as shown in Fig. 5 of the Supplemental Material [49]. In this scenario, the inverted gap and the Fermi wave vector are almost unchanged, incompatible with the transport results. Therefore, we attribute the anomaly in FS and phase factor in Cd_3As_2 under high pressure to be an anisotropic-compression-induced band-gap opening. Here we assume that the temperature difference between transport and XRD experiments does not strongly affect the anomalous transition, except for the slight variation in critical pressure value.

Apart from the gap opening and node-pair annihilation discussed above, there are other mechanisms that may lead to a change of the phase factor. Firstly, a field-induced phase shift has been observed in Cd_3As_2 [3,11]. High magnetic field deviating from the fourfold rotational axis will generate a hybridization gap and therefore affect the phase factor [11]. The unique characteristic of this effect is that the phase factor changes gradually with $\boldsymbol{B}$, while the field along the rotational axis will have no such effect. Here in this study, the magnetic field is perpendicular to the (112) plane. As reported earlier [3],

the field along this direction will have a significant impact only when it is larger than 7 T. In the fitting process of the Landau fan diagram [Fig. 2(d)], most of the points are from the low-field regime (below 6 T). We also compared the phase factor extracted from the low-field regime (Fig. 6 of the Supplemental Material [49]). No such field dependence is observed, thus excluding the magnetic field as the origin of the phase shift. Another possible reason could be an anomalous phase shift which emerges near the Lifshitz point as proposed by Wang *et al.* recently [51]. In either the linear or parabolic limit, the energy spectrum is a simple function of k_z^2 with ± 0.125 phase shift compared with that in two dimensions. Away from these two limits, this simple k_z^2 dependence is violated and it leads to a nonmonotonic change in the phase shift [51]. Near the Lifshitz transition point, with a considerable component of the parabolic dispersion, this phase shift could be relatively large [51]. Meanwhile, an additional beating pattern may be observed due to the Landau level crossing at extreme points of the band structure [51]. As shown in Fig. 2(c), the Fermi vector given by the SdH oscillations suggests that the Fermi level is well above the Lifshitz energy ($\sim$20 meV) given by our calculations and also previous experiments [12]. Additionally, the Lifshitz energy further decreases with c/a ratio [refer to Fig. 4(f)]. Moreover, the extracted SdH oscillations show a clear single frequency, with no sign of a beating pattern. Hence, although we do not fully deny its existence, the present experimental evidences do not support the band extreme point as a dominant contribution to the observed phase shift. Furthermore, the single-band oscillations also rule out other scenarios like the Zeeman splitting or a second band.

III. CONCLUSION

To conclude, we have reported a detailed study of Cd_3As_2 under pressure. Apart from the monoclinic structure transition, we observe signatures of another possible phase transition around 1.3 GPa, as indicated by the anomalous behavior in the FS and the phase factor. Combined with band structure calculations, we find that an anisotropic compression will annihilate the Dirac nodes and induce a finite gap. Our result calls for further investigations into the anomalous compression behavior of crystal and electronic structure in Cd_3As_2.

[1] B. J. Yang and N. Nagaosa, Nat. Commun. **5**, 4898 (2014).

[2] Z. K. Liu, B. Zhou, Y. Zhang, Z. J. Wang, H. M. Weng, D. Prabhakaran, S. K. Mo, Z. X. Shen, Z. Fang, X. Dai, Z. Hussain, and Y. L. Chen, Science **343**, 864 (2014).

[3] J. Cao, S. Liang, C. Zhang, Y. Liu, J. Huang, Z. Jin, Z. G. Chen, Z. Wang, Q. Wang, J. Zhao, S. Li, X. Dai, J. Zou, Z. Xia, L. Li, and F. Xiu, Nat. Commun. **6**, 7779 (2015).

[4] B.-J. Yang, E.-G. Moon, H. Isobe, and N. Nagaosa, Nat. Phys. **10**, 774 (2014).

[5] K. Landsteiner, Y. Liu, and Y. W. Sun, Phys. Rev. Lett. **116**, 081602 (2016).

[6] H. Isobe, B. J. Yang, A. Chubukov, J. Schmalian, and N. Nagaosa, Phys. Rev. Lett. **116**, 076803 (2016).

[7] C. Z. Chen, J. Song, H. Jiang, Q. F. Sun, Z. Wang, and X. C. Xie, Phys. Rev. Lett. **115**, 246603 (2015).

[8] S. Bera, J. D. Sau, and B. Roy, Phys. Rev. B **93**, 201302(R) (2016).

[9] R. Okugawa and S. Murakami, Phys. Rev. B **89**, 235315 (2014).

[10] H. Pan, M. Wu, Y. Liu, and S. A. Yang, Sci. Rep. **5**, 14639 (2015).

[11] Z. J. Xiang, D. Zhao, Z. Jin, C. Shang, L. K. Ma, G. J. Ye, B. Lei, T. Wu, Z. C. Xia, and X. H. Chen, Phys. Rev. Lett. **115**, 226401 (2015).

[12] S. Jeon, B. B. Zhou, A. Gyenis, B. E. Feldman, I. Kimchi, A. C. Potter, Q. D. Gibson, R. J. Cava, A. Vishwanath, and A. Yazdani, Nat. Mater. **13**, 851 (2014).

[13] A. Jayaraman, Rev. Mod. Phys. **55**, 65 (1983).

[14] P. Gegenwart, Q. Si, and F. Steglich, Nat. Phys. **4**, 186 (2008).

[15] J. Paglione and R. L. Greene, Nat. Phys. **6**, 645 (2010).

[16] J. Zhang, F.-L. Liu, J.-K. Dong, Y. Xu, N.-N. Li, W.-G. Yang, and S.-Y. Li, Chin. Phys. Lett. **32**, 097102 (2015).

[17] Y. Luo, N. Ghimire, E. Bauer, J. Thompson, and F. Ronning, J. Phys.: Condens. Matter **28**, 055502 (2016).

[18] Y. Zhou, P. Lu, Y. Du, X. Zhu, G. Zhang, R. Zhang, D. Shao, X. Chen, X. Wang, M. Tian, J. Sun, X. Wan, Z. Yang, W. Yang, Y. Zhang, and D. Xing, Phys. Rev. Lett. **117**, 146402 (2016).

[19] R. D. dos Reis, S. C. Wu, Y. Sun, M. O. Ajeesh, C. Shekhar, M. Schmidt, C. Felser, B. Yan, and M. Nicklas, Phys. Rev. B **93**, 205102 (2016).

[20] S. Zhang, Q. Wu, L. Schoop, M. N. Ali, Y. Shi, N. Ni, Q. Gibson, S. Jiang, V. Sidorov, W. Yi, J. Guo, Y. Zhou, D. Wu, P. Gao, D. Gu, C. Zhang, S. Jiang, K. Yang, A. Li, Y. Li *et al.*, Phys. Rev. B **91**, 165133 (2015).

[21] H. Wang, H. Wang, H. Liu, H. Lu, W. Yang, S. Jia, X.-J. Liu, X. Xie, J. Wei, and J. Wang, Nat. Mater. **15**, 38 (2016).

[22] L. Aggarwal, A. Gaurav, G. S. Thakur, Z. Haque, A. K. Ganguli, and G. Sheet, Nat. Mater. **15**, 32 (2016).

[23] L. He, Y. Jia, S. Zhang, X. Hong, C. Jin, and S. Li, npj Quantum Mater. **1**, 16014 (2016).

[24] A. Narayanan, M. D. Watson, S. F. Blake, N. Bruyant, L. Drigo, Y. L. Chen, D. Prabhakaran, B. Yan, C. Felser, T. Kong, P. C. Canfield, and A. I. Coldea, Phys. Rev. Lett. **114**, 117201 (2015).

[25] L. P. He, X. C. Hong, J. K. Dong, J. Pan, Z. Zhang, J. Zhang, and S. Y. Li, Phys. Rev. Lett. **113**, 246402 (2014).

[26] T. Liang, Q. Gibson, M. N. Ali, M. Liu, R. J. Cava, and N. P. Ong, Nat. Mater. **14**, 280 (2014).

[27] C. Zhang, E. Zhang, W. Wang, Y. Liu, Z.-G. Chen, S. Lu, S. Liang, J. Cao, X. Yuan, L. Tang, Q. Li, C. Zhou, T. Gu, Y. Wu, Z. Jin, and F. Xiu, Nat. Commun. **8**, 13741 (2017).

[28] Z.-G. Chen, C. Zhang, Y. Zou, E. Zhang, L. Yang, M. Hong, F. Xiu, and J. Zou, Nano Lett. **15**, 5830 (2015).

[29] Z. J. Xiang, G. J. Ye, C. Shang, B. Lei, N. Z. Wang, K. S. Yang, D. Y. Liu, F. B. Meng, X. G. Luo, L. J. Zou, Z. Sun, Y. Zhang, and X. H. Chen, Phys. Rev. Lett. **115**, 186403 (2015).

[30] J. Anderson, W. O'Sullivan, and J. Schirber, Phys. Rev. **153**, 721 (1967).

[31] P. L. Cai, J. Hu, L. P. He, J. Pan, X. C. Hong, Z. Zhang, J. Zhang, J. Wei, Z. Q. Mao, and S. Y. Li, Phys. Rev. Lett. **115**, 057202 (2015).

[32] W. B. Holzapfel, Rep. Prog. Phys. **59**, 29 (1996).

[33] M. Neupane, S.-Y. Xu, R. Sankar, N. Alidoust, G. Bian, C. Liu, I. Belopolski, T.-R. Chang, H.-T. Jeng, and H. Lin, Nat. Commun. **5**, 3786 (2014).

[34] S. Borisenko, Q. Gibson, D. Evtushinsky, V. Zabolotnyy, B. Büchner, and R. J. Cava, Phys. Rev. Lett. **113**, 027603 (2014).

[35] J. Feng, Y. Pang, D. Wu, Z. Wang, H. Weng, J. Li, X. Dai, Z. Fang, Y. Shi, and L. Lu, Phys. Rev. B **92**, 081306 (2015).

[36] D. Xiao, M.-C. Chang, and Q. Niu, Rev. Mod. Phys. **82**, 1959 (2010).

[37] G. P. Mikitik and Y. V. Sharlai, Phys. Rev. Lett. **82**, 2147 (1999).

[38] J. H. Bardarson and J. E. Moore, Rep. Prog. Phys. **76**, 056501 (2013).

[39] A. R. Wright and R. H. McKenzie, Phys. Rev. B **87**, 085411 (2013).

[40] A. A. Taskin and Y. Ando, Phys. Rev. B **84**, 035301 (2011).

[41] W. Desrat, C. Consejo, F. Teppe, S. Contreras, M. Marcinkiewicz, W. Knap, A. Nateprov, and E. Arushanov, J. Phys.: Conf. Ser. **647**, 012064 (2015).

[42] A. Akrap, M. Hakl, S. Tchoumakov, I. Crassee, J. Kuba, M. O. Goerbig, C. C. Homes, O. Caha, J. Novak, F. Teppe, W. Desrat, S. Koohpayeh, L. Wu, N. P. Armitage, A. Nateprov, E. Arushanov, Q. D. Gibson, R. J. Cava, D. van der Marel, B. A. Piot *et al.*, Phys. Rev. Lett. **117**, 136401 (2016).

[43] M. Orlita, D. M. Basko, M. S. Zholudev, F. Teppe, W. Knap, V. I. Gavrilenko, N. N. Mikhailov, S. A. Dvoretskii, P. Neugebauer, C. Faugeras, A. L. Barra, G. Martinez, and M. Potemski, Nat. Phys. **10**, 233 (2014).

[44] J. D. Malcolm and E. J. Nicol, Phys. Rev. B **92**, 035118 (2015).

[45] H. Murakawa, M. S. Bahramy, M. Tokunaga, Y. Kohama, C. Bell, Y. Kaneko, N. Nagaosa, H. Y. Hwang, and Y. Tokura, Science **342**, 1490 (2013).

[46] G. Kresse and J. Furthmüller, Comput. Mater. Sci. **6**, 15 (1996).

[47] J. P. Perdew, K. Burke, and M. Ernzerhof, Phys. Rev. Lett. **77**, 3865 (1996).

[48] Z. Wang, H. Weng, Q. Wu, X. Dai, and Z. Fang, Phys. Rev. B **88**, 125427 (2013).

[49] See Supplemental Material at http://link.aps.org/supplemental/10.1103/PhysRevB.96.155205 for material growth and characterizations, supporting transport data, band structure calculations, and theoretical model of Dirac node annihilation.

[50] A. Narayan, D. Di Sante, S. Picozzi, and S. Sanvito, Phys. Rev. Lett. **113**, 256403 (2014).

[51] C. M. Wang, H.-Z. Lu, and S.-Q. Shen, Phys. Rev. Lett. **117**, 077201 (2016).